ISBN: 978-3-95450-132-8 doi:10.18429/JACoW-IPAC2014-THPRO020

LINAC LATTICE OPTIMIZATION FOR PAL-XFEL HARD X-RAY FEL LINE*

H. Yang#, J. H. Han, H. -S. Kang, I. S. Ko ,
Pohang Accelerator Laboratory, Pohang 790-784, Korea

Abstract

PAL-XFEL is designed to generate 1 – 0.06-nm FEL in hard x-ray FEL line. The linac for hard x-ray generates 10-GeV, 200-pC, and 3-kA electron beam. It consists of accelerating columns, three bunch compressors, an X-band linearizer, and dog-leg line. We conduct ELEGANT simulations to obtain the optimized lattice for hard x-ray line. The candidates of the optimized lattice are obtained by Multi-Objective Genetic Algorithm (MOGA) whose objectives are the FEL saturation power and length. These are evaluated with their error tolerances. Error tolerances are obtained by two methods of error simulations. First, the linear interpolation method is conducted in order to determine the machine tolerance. Also, we find out the dominant machine parameters to increase the beam jitter by this method. Second, the error simulations with random errors of machine parameters are conducted to verify the results of the linear interpolation method and calculate beam jittering levels. In this paper, we present the details of the optimized linac lattice for hard x-ray FEL. Also, we present the procedure of the linac lattice optimization.

INTRODUCTION

PAL-XFEL is designed to provide 1–0.06-nm hard x-ray (HX) FEL and 10–1-nm soft x-ray (SX) FEL [1]. The linac for HX generates 10-GeV, 200-pC, and 3-kA electron beam (Table 1). The HX linac lattice consists of four sections of accelerating columns, three bunch compressors, an X-band linearizer, and dog-leg line (Fig. 1). In the XFEL system, both of the FEL power and stability are significant for user experiments. Then, the system should be optimized for high power of FEL and the beam stability studies are required alike other FEL machines [2, 3]. The FEL performance is determined by electron beam parameters from the linac and undulator conditions. Since the undulator parameters are static, dynamic FEL errors are arisen by electron beam jitters which are arisen by machine errors in the linac.

We conducted optimization of HX linac lattice for PAL-XFEL by Multi-Objective Genetic Algorithm (MOGA) optimizer with ELEGANT. MOGA is a powerful tool to optimize problems with large number of variables and objectives. Accordingly, it was used in other accelerator systems [4, 5]. In our optimization, objectives are the saturation power and length, and constraints are the slice emittances. The optimized linac lattice was selected among the high ranks of MOGA result according to some constraints.

*Work supported by MSIP, Korea.
#highlong@postech.ac.kr

We conducted error simulations for machine tolerance studies to evaluate the lattice stability. Two methods were conducted. The first is linear interpolation method [6]. From this method, we not only determined the machine tolerances but also identified the dominant machine parameters to arise electron beam jitter. The second is error simulations with random errors of machine. It was conducted to verify the machine tolerances from the first method. Also, we calculated the electron beam jittering levels by various machine errors. In this paper, we discuss and organize the sequence of linac lattice optimization and evaluation.

Table 1: Parameters for Hard X-ray FEL

Parameters (unit)	Values
Beam energy (GeV)	10
Beam charge (nC)	0.2
Slice emittance (mm-mrad)	0.4
Injector gun	Photocathode RF-gun
Peak current at undulator (kA)	3.0
Repetition rate (Hz)	60
Linac structure	S-band
Undulator type	Out-vacuum
Hard x-ray wavelength (nm)	1 ~ 0.06
Photon flux @ 0.1 nm, photons/pulse	> 1.0 E+12

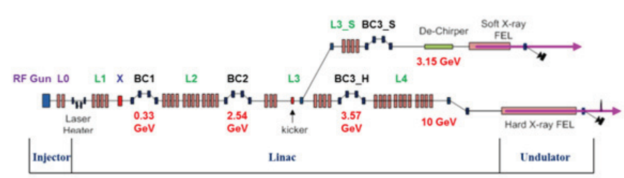

Figure 1: Schematic diagram of PAL-XFEL. The soft x-ray line is branched at the middle of L3.

LINAC LATTICE OPTIMIZATION

We optimized the HX linac lattice by the MOGA optimizer whose script was written by M. Borland and H. Shang [7]. We used 4 best children to generate 16 next generations. Objectives are saturation power and length, and constraints are the horizontal and vertical slice emittances [8]. Ming Xie formula was used to calculate the saturation power and length. For reducing simulation time, we fixed some variables. The longitudinal position and length of all elements were fixed. β-functions matching with quadrupole magnets were conducted by the simplex optimization in ELEGANT. In addition, the accelerating gradients of the linac sections were fixed and the RF phase of the X-band linearizer was fixed on -180°.

ISBN: 978-3-95450-132-8 doi:10.18429/JACoW-IPAC2014-THPRO020

MOGA with 8 variables (Fig. 2) ranks all simulation sets by the objectives and constraints.

We determined the optimized linac lattice among the high ranks of MOGA. It is the lattice of highest saturation power according to constraints as follows:

- The current profile is flat in core slices
- Preventing over current of head and tail
- Under 3-kA peak current at the end of linac
- Under 0.6-kA peak current at the end of BC2

This linac lattice is able to generate 10-GeV, 200-pC, and 2.9-kA electron beam with 65-fs bunch length, 0.42-µm horizontal normalized projected emittance, and 0.26-µm vertical normalized projected emittance (Table 2). The saturation power is 12 GW and the saturation length is about 53 m from Ming Xie formula with undulator period of 21.4-mm and undulator K of 1.516. The energy spread of the slice core is maintained in ±0.02% and the horizontal and vertical slice emittances are under 0.3-um (Fig. 3(a), (b)). The current distribution is single horn shape (Fig. 3(c)). The horizontal β-function is minimized at the end of bunch compressors for suppressing the emittance dilution (Fig. 4).

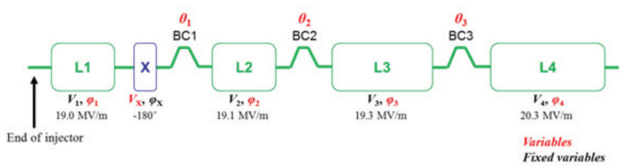

Figure 2: Schematic diagram of the hard x-ray linac lattice for PAL-XFEL and variables of the MOGA optimization.

Table 2: Machine Parameters of HX line for PAL-XFEL

Parameters (unit)	Values
Beam energy (GeV)	10.04
Beam charge (pC)	200
Peak beam current (kA)	2.91
Bunch length (fs)	65
Normalized projected emittance_H (µm)	0.423
Normalized projected emittance_V (µm)	0.263
Saturation power (GW)	12.0
Saturation length (m)	52.8

MACHINE ERROR TOLERANCE

Linear Interpolation Method

The constraint for the machine tolerances of the linac is represented by [6]

$$\sqrt{\sum_{i=1}^{N}\left\{\frac{\sigma(\Delta x_i/x_{i0})}{P_{sen}}\right\}^2} < 1\,, \qquad (1)$$

,where, f is beam parameter, x is machine parameter, $P_{sen} = T/[\partial(f/f_0)/\partial(\Delta x_i/x_{i0})]$, and T is target value of the beam tolerance.

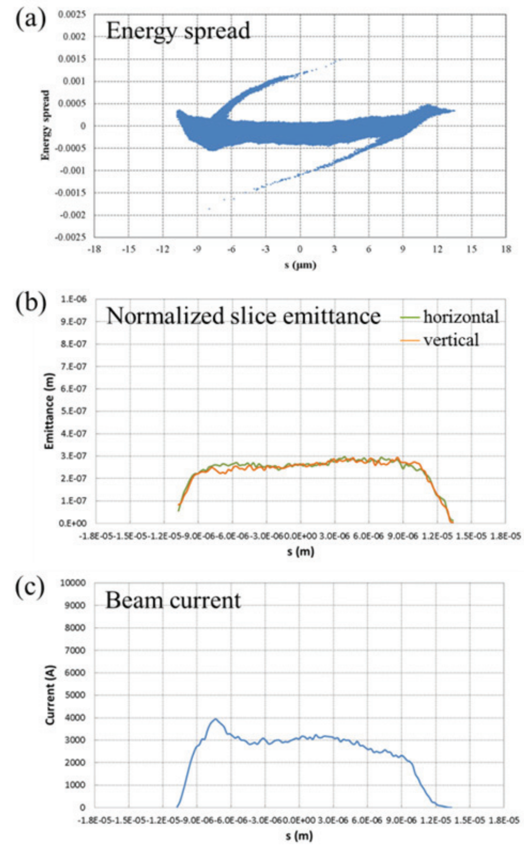

Figure 3: (a) Energy spread, (b) Normalized slice emittance of horizontal (green) and vertical (orange), and (c) current of electron beams at the end of the linac in the optimized linac lattice.

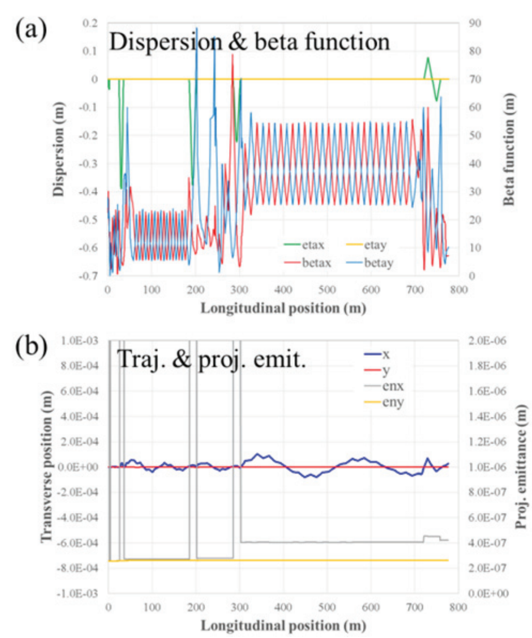

Figure 4: (a) Dispersions (green, yellow) and β-functions (red, cyan), and (b) beam trajectories (blue, red) and variation of the normalized projected emittances (gray, yellow) in the optimized linac lattice.

ISBN: 978-3-95450-132-8 doi:10.18429/JACoW-IPAC2014-THPRO020

The beam tolerances were determined under ±10% of the current variation, ±0.02% of the energy variation, ±20 fs of the arrival time variation, and 10% of the horizontal normalized projected emittance variation. The machine parameters are the phase and voltage of RF structures, and the bending angle of dipoles in bunch compressors (Table 3). The partial derivatives of variations of beam parameters versus variations of machine parameters were obtained by the linear interpolation of ELEGANT results.

Table 4 is the machine tolerances (M) determined with Eq. (1). Since the machine tolerance is loosened by multi-klystrons, $\sigma(x_i) = \sqrt{N}\sigma(x)$ were applied, where N is the number of klystrons. $\sum[M/P_{sen}]^2$ should be lower than 1 in Eq. (4), but 0.44 were remained considering other variables like the gun timing jitter and the charge jitter in the injector (Table 4) [6]. The machine tolerances were determined to maintain $\sum[M/P_{sen}]^2 < 0.5$, and they are little tight but achievable values with the available technology. Also, it was verified that the RF phase and voltage of the L1 and L2, and the RF phase of the X-band linearizer are dominant parameters to arise beam jitters.

Table 3: Machine Parameters of HX Linac Lattice

Elements	Variables (linac)
RF structures (L1 ~ L4, X)	phase (φ_1, φ_2, φ_3, φ_4, φ_X) voltage (V_1, V_2, V_3, V_4, V_X)
Bends (BC1~3)	bending angle (θ_1, θ_2, θ_3)

Table 4: Machine Tolerances of HX Linac Lattice

$[M/P_{sen}]^2$

Parameter	# of klystron	sym bol	$\Delta I/I_0 =$ ±10%	$<\Delta E/E_0> =$ ±0.02%	$\Delta t_f =$ ±20fs	$\Delta\varepsilon_{nx}/\varepsilon_{nx0}$ = ±10%	Tolerance (rms)	unit
Mean L1 rf phase	2	φ_1	0.0897	0.0001	0.1215	0.0840	**0.03**	deg.
Mean X rf phase	1	φ_X	0.3084	0.0185	0.0004	0.3637	**0.07**	deg.
Mean L2 rf phase	10	φ_2	0.0069	0.0050	0.0996	0.0071	**0.03**	deg.
Mean L3 rf phase	4	φ_3	0.0001	0.0000	0.0000	0.0001	**0.1**	deg.
Mean L4 rf phase	27	φ_4	0.0000	0.0000	0.0000	0.0000	**0.1**	deg.
Mean L1 rf voltage	2	V_1	0.0094	0.0049	0.0425	0.0055	**0.01**	%
Mean X rf voltage	1	V_X	0.0035	0.0020	0.0218	0.0001	**0.05**	%
Mean L2 rf voltage	10	V_2	0.0003	0.0053	0.1879	0.0004	**0.02**	%
Mean L3 rf voltage	4	V_3	0.0000	0.0135	0.0201	0.0001	**0.05**	%
Mean L4 rf voltage	27	V_4	0.0000	0.0994	0.0000	0.0000	**0.05**	%
B.C.-1 angle	-	θ_1	0.0001	0.0000	0.0000	0.0001	**0.002**	%
B.C.-2 angle	-	θ_2	0.0000	0.0000	0.0000	0.0000	**0.002**	%
B.C.-3 angle	-	θ_3	0.0000	0.0000	0.0000	0.0000	**0.002**	%
Sum			0.4185	0.1487	0.4937	0.4612		

*__0.44__ is portion for unconsidered variable

Random Error Simulation

Since machine errors are arisen randomly in the real operation condition, it is required to verify the machine tolerances by random error simulations. This simulation method could calculate the beam jittering level from the applied machine errors. The machine tolerances obtained by the previous method were applied in Case 1 and the relatively loosened tolerances were applied in Case 2 (Table 5). Table 6 is the beam jittering levels of two cases and both of them achieve the target values.

Table 5: Error Setting of Random Error Simulations

Element	rms errors (Gaussian, 3-σ cutoff)	Value #1	Value #2	Unit
RF struc.	phase errors	0.03 (L1) 0.07 (X) 0.03 (L2) 0.1 (L3~4)	0.05 (L1) 0.1 (X) 0.05 (L2) 0.1 (L3~4)	deg.
	relative voltage errors	100 (L1) 400 (X) 200 (L2) 500 (L3~4)	200 (L1) 400 (X) 200 (L2) 1000 (L3~4)	ppm
Bends	bending angle errors	20	20	ppm
Drift	length errors (→ timing errors)	10 (66)	10 (66)	μm (*fs*)
e^- beam	random charge error	1	1	%

Table 6: Beam Jitters by Random Machine Errors

Beam jitter (standard deviation)	$\Delta I/I_0$	$\Delta E/E_0$	Δt_f	$\Delta\varepsilon_{nx}/\varepsilon_{nx0}$
Target	10%	0.02%	20 *fs*	10%
Case 1	8.7%	0.009%	14.0 *fs*	6.5%
Case 2	10.1%	0.015%	19.1 *fs*	8.1%

SUMMARY

We optimized HX linac lattice for PAL-XFEL with MOGA. The optimized lattice was determined among high ranks of MOGA according to some constraints, and it was designed to generate 10-GeV, 200-pC, and 2.9-kA electron beam with 65-fs bunch length, 0.42/0.26-μm projected emittance. The machine error simulations were conducted to evaluate machine tolerances. They were obtained by the linear interpolation method, and achieved the beam tolerances under ±10% of the current variation, ±0.02% of the energy variation, ±20 fs of the arrival time variation, and 10% of the projected emittance variation. The obtained machine tolerances were confirmed by random error simulations. As a result, the optimized linac lattice was verified to achieve targets of beam jitters with achievable machine tolerances.

REFERENCES

[1] H. S. Kang, et al., in: Proceedings of IPAC2012, New Orleans, Louisiana, USA (2012) 1738.

[2] R. Akre, et al., in: Proceedings of FEL2008, Gyeongju, Korea (2008) 94.

[3] S. Reiche and P. Scherrer., in Proceedings of FEL2009, Liverpool, UK (2009) 643.

[4] L. Emery, in: Proceedings of PAC2005, Knoxville, Tennessee, USA (2005) 2962.

[5] R. Bartolini, et al., Physical Review Special Topics – Accelerators and Beams 15 (2012) 030701.

[6] J. Arthur et al., Conceptual Design Report: Linac Coherent Light Source (LCLS), SLAC–R–593, April 2002.

[7] K. Deb, et al., IEEE Transactions on Evolutionary Computation 6 (2002) 182.

[8] C. H. Yi, et al., in: Proceedings of IPAC2012, New Orleans, Louisiana, USA (2012) 1224.